Specificity of Measuring Thermal Resistance in Solar Cells

Vitaliy Ivanovich Smirnov, Viacheslav Andreevich Sergeev, and Andrey Anatolievich Gavrikov

***Abstract*—This paper describes a modulation method of measuring the thermal impedance of solar modules. The measurements are taken by varying heating power harmonically and measuring a variable component of the junction temperature, which changes in response to it. Analyzing the dependence of thermal impedance on modulation frequency allows the determination of thermal impedance components corresponding to the structural elements of a solar module. It is experimentally shown that the amplitude of the variable component of junction temperature is mostly independent of the value of the heating power. This is explained by current crowding, that is a nonuniform distribution of the current through the junction and formation of local heating areas of the semiconductor. The formation of local heating areas is confirmed by the experimentally detected thermal resistance component, which takes place due to the temperature difference between local heating areas and the other part of a semiconductor of a solar module. Another confirmation of the local heating areas is a sharp thermal resistance decrease with an increase in the heating current.**

***Index Terms*—Photovoltaic cells, thermal analysis, thermal resistance.**

I. Introduction

THE efficiency of Si-based solar modules is usually approximately 12–28% [1]. This means that more than 70% of the light energy absorbed by the module is converted to heat. With a temperature increase of 1 °C, the nominal power of solar modules is reduced by approximately 0.4%, so the resulting power reduction of the modules can reach 15–25% [2]. At temperatures above 100–125 °C, they can temporarily lose the capacity to work, and higher temperatures can irreversibly damage them. In addition, the increased temperature accelerates solar modules' degradation. Thus, requirements on the quality of a solar module heat sink are very strict.

Heat removal from a semiconductor to surroundings can be implemented in three ways: convection, thermal radiation, and conduction. The efficiency of heat dissipation due to convection depends on external conditions, primarily on the ambient temperature and the airflow velocity where the module is placed [3]. The power of thermal radiation is determined by the temperature of the radiating object, i.e., semiconductor plates of the module. The efficiency of heat dissipation by conduction is determined by the design of the module and its manufacturing technology, primarily by the substrate thermal conductivity and by the quality of the thermal contact between the substrate and semiconductor.

The quality of the thermal contact between the semiconductor and the substrate depends on thermal resistance R_T "junction-to-case," defined as follows:

$$R_{Tjx} = \frac{T_j - T_x}{P} = \frac{\Delta T_j}{P} \tag{1}$$

where T_J is the p-n junction temperature in a steady-state test condition; T_X is the reference temperature of the case or surroundings; and *P* is dissipated power.

Lower thermal resistance, R_{Tjx}, between the p-n junction and the module case (substrate) corresponds to lower temperature of the semiconductor dies and higher output power of the solar module. Despite the importance of measuring the thermal resistance of solar modules, there are no standards for measuring thermal resistance of solar modules and the number of publications on the topic is very low [1], [3]–[6].

Siegel's important work on the topic [1] suggests that solar cells can be considered as a set of diodes connected in series and in parallel. This makes it possible to use thermal transient testing [7] for measuring the thermal resistance of solar cells. In this case, the device under test (DUT) is heated by passing pulses of forward current, I_h. The p-n junction temperature, T_j, is determined indirectly and based on a forward voltage drop on the junction at low measuring current I_m, which is a temperature-sensitive parameter (TSP); the forward voltage drop is linearly related to the junction temperature. The ambient light surrounding the thermal measurement setup should be kept to a minimum. Otherwise, the cell becomes a source of electrical energy as well as an electrical power dissipater. At the same time, the heating current must be large enough to heat the junction by at least 20 °C [1]. Otherwise, the accuracy of the thermal resistance measurements will not be high enough.

In Zhang *et al.*'s work [4], the object of the study was a solar cell with a surface area of approximately 16 cm^2. The value of the heating current, I_h, varied from 100 to 700 mA. It was found that as I_h increased, the thermal resistance of the R_T

Manuscript received October 6, 2018; revised November 19, 2018; accepted January 31, 2019. Date of publication March 5, 2019; date of current version April 19, 2019. This work was supported by the Russian Foundation for Basic Research and Government of Ulyanovsk region (Project no. 18-48-730018). *(Corresponding author: Andrey Anatolievich Gavrikov.)*

V. I. Smirnov, V. A. Sergeev are with the Ulyanovsk Branch of the Institute of Radioengineering and Electronics, Russian Academy of Science, Ulyanovsk 432071, Russia, and also with the Ulyanovsk State Technical University, Ulyanovsk 432027, Russia (e-mail: smirnov-vi@mail.ru; sva@ulstu.ru).

A. A. Gavrikov is with the Ulyanovsk Branch of the Institute of Radioengineering and Electronics, Russian Academy of Science, Ulyanovsk 432071, Russia (e-mail: a.gavrikoff@gmail.com).

Color versions of one or more of the figures in this paper are available online at http://ieeexplore.ieee.org.

Digital Object Identifier 10.1109/JPHOTOV.2019.2897349

solar cell decreased from 28.5 to 3 K/W, and the dependence of R_T on the heating current, I_h, is nonlinear. The value of R_T decreases sharply in the current range from 100 to 300 mA and is practically constant at $I_h > 300$ mA. This result was, however, not explained by the authors.

The nonlinear dependency of solar cell thermal resistance, R_T, on the magnitude of the heating current, I_h, is confirmed in the studies, summarized by Plesz *et al*. [5]. Plesz *et al.* also proposed an explanation for the sharp decrease in the solar cells' thermal resistance with increasing magnitude of the heating current. A possible explanation for this phenomenon is current crowding. In the case of lower heating currents, the p-n junction forward current is not distributed homogeneously along the device surface, but rather causes dissipation only in some areas of the device. As heating current increases, more and more areas of the p-n junction reach the forward opening voltage and start to dissipate power; thus, the heat path is extended resulting in a lower thermal resistance.

In many studies [1], [3]–[6], solar cell and solar module thermal resistance measurements were based on the JESD51 1-14 standard [7], which implies heating the DUT by stepping power changes and measuring the response, which is the change in junction temperature, T_j(t), with respect to the initial temperature, $T_j(t = 0)$. This standard is implemented by the thermal transient tester measuring device manufactured by Mentor Graphics, Ltd [8]. It is necessary to maintain a constant DUT temperature; that is why thermal transient testing was done in a dual mount for cold plate measurements, keeping both the front and back surfaces of the solar cell at 25 °C. A solar panel, with a power of tens and hundreds of watts, has a significantly larger surface than the sizes of cold plates currently manufactured [9]. This makes it impossible to maintain the temperature of the case for such objects.

The aim of this research was to develop a method for measuring thermal resistance components of an efficient large-sized solar module and to determine the influence of the heating current value on the measurement results.

II. Modulation Method for Measuring Thermal Resistance

For measuring the thermal resistance of large-sized solar modules, a modulation measurement method [10, 11] is used. In contrast to the JESD51 1-14 standard, the DUT is heated using harmonically varied heating power. A pulse sequence of heating current, with the pulse length varying harmonically, is passed through the DUT

$$\tau_p(t) = \tau_{p\_\mathrm{avg}}(1 + a \cdot \sin 2\pi\nu t) \tag{2}$$

where τ_{p_avg} is the average pulse length; a is the modulation factor of the heating power; and ν is the modulation circular frequency. The average value of the heating power for a pulse period, $\bar{P}(t)$, also varies harmonically

$$\begin{aligned} P(t) &= I_h U_h \frac{\tau_p(t)}{T_p} = I_h U_h \frac{\tau_{p\_\mathrm{avg}}}{T_p}(1 + a \cdot \sin\, 2\pi\nu t) \\ &= P_0 + P_1 \cdot \sin\, 2\pi\nu t \end{aligned} \tag{3}$$

where U_h is the voltage at the top of the heating pulses; P_0 is the constant component of power; P_1 is the amplitude of the changing component of heating power, ($P_1 < P_0$), and I_h is heating current.

The p-n-junction temperature after each heating pulse is determined based on the TSP measurements taken in the pauses between heating pulses, with a little time delay with respect to pulse edges. This delay is necessary for finishing transitional electrical processes. For the DUT, the time delay was 240 μs. The TSP measurement starts after a short DUT preheating to arrive at the thermal condition where the junction temperature fluctuates with respect to a quasi-stationary value of $T(t)$, which varies with the modulation frequency of the heating power

$$T(t) = T_0 + T_1 \cdot \sin(2\pi\nu t - \phi) \tag{4}$$

where T_0 is the constant component of the junction temperature; T_1 is the amplitude of the variable component of the junction temperature at the modulation frequency, and φ is the phase shift between the variable components of the junction temperature and the heating power.

The $T(\nu)$ spectrum is calculated by Fourier transform and then digitally filtered. After that, the combined dependence $T(t)$ is restored. The signal was filtered in frequency domain using a low-pass filter by multiplying temperature Fourier transforms $T(\nu)$ by rectangular filter function. The width of the rectangular filter was three times higher than the first harmonic frequency. The thermal impedance magnitude, $Z_T(\nu)$, on the modulation frequency, ν, is determined by the ratio of the amplitudes of the variable components of the junction temperature, T_1, and power, P_1. Thermal impedance phase is determined by the ratio of the real and imaginary Fourier transforms, $A_1(\omega)$ and $B_1(\omega)$, at the modulation frequency.

Thermal resistance components are measured based on the frequency dependencies of magnitude, $Z_T(\nu)$, phase, $\varphi(\nu)$, and the real part of thermal impedance, Re $Z_T(\nu)$. They have peculiarities such as flat graph sections or inflexion points corresponding to various thermal resistance components. To identify such peculiarities, the derivatives of these values are determined by modulation frequency. According to Smirnov *et al.* [11], the analysis of the Re $Z_T(\nu)$ frequency dependence gives more accurate results.

III. Research Materials and Experiment Conditions

The device used in this research was a polycrystalline silicon solar module Sunways FSM 50P. The total surface area of the module was 700 × 550 mm^2, the total power was 50 W, the voltage at maximum power (Vmp) is 18.0 V, voltage at open circuit (Voc) is 23.6 V, current at max power (Imp) is 2.78 A.

The module is made according to a common design: Polycrystalline silicon cells are fixed on a plate of tempered glass, covered with a protective ethylene vinyl acetate film from the back and attached to the aluminium frame.

Thermal resistance was measured using the pulse characterograph of semiconductor devices [9], [11] (meter), shown in Fig. 1, which uses the modulation method.

Fig. 1. General view of a thermal impedance meter.

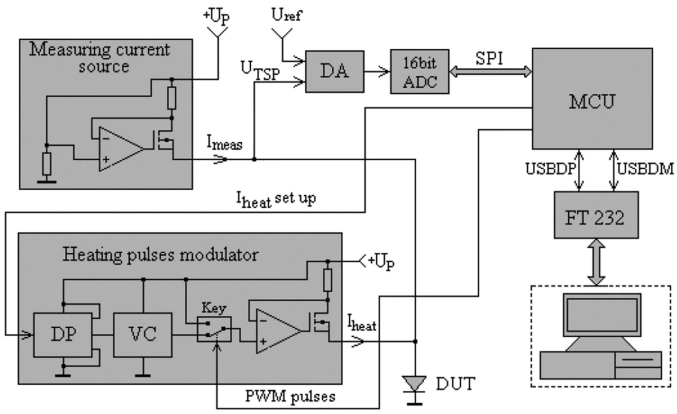

Fig. 2. Thermal impedance meter functional diagram.

For the meter, the measurement range of thermal resistance is 0.01–100 K/W; the measurement error is 5%; the heating current range is 0.25–4 A; and the frequency range of the heating power modulation is 0.01–1000 Hz.

The repetition period of the heating pulses was 1000 μs; the pulse length was modulated from 250 to 750 μs; and the heating current pulse amplitude, I_h, was set in the range of 250–2500 mA. During the measurements, the module was in a light-proof casing (in Fig. 1, the module is without the casing). No special actions were performed to maintain the temperature of the module case because the temperature of the DUT's case does not significantly affect the measurement results in comparison with thermal transient testing [7]. This is illustrated by the example of a power MOSFET and insulated-gate bipolar transistor (IGBT) transistors [12].

The meter functional diagram is depicted in Fig. 2 [10]. It is controlled using a microcontroller (MCU). The heating pulse generator is based on an operational amplifier (OA) with MOSFET in a feedback circuit.

The measuring current value, $I_{\rm meas}$, is determined by the voltage between the OA noninverted pin and the voltage driving resistor in the transistor's drain circuit. The heating current pulse-shaping circuit works in a similar way, but the voltage on the OA noninverted pin is set by the MCU with a digital potentiometer and a voltage level converter.

The pulse-shaping circuit scheme eliminates the influence of parameter variations of a field transistor that are caused by its heating by heavy currents. The pulse-width modulation of heating pulses is accomplished with the switch (Key).

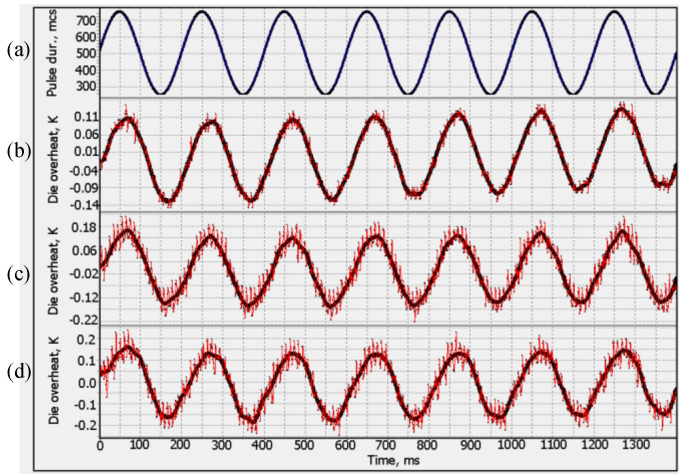

Fig. 3. (a) Time dependencies of the heating pulse duration. The variable component of the junction temperature at (b) $I_h = 250$ mA, (c) $I_h = 1000$ mA, and (d) $I_h = 2000$ mA.

The voltage drop (TSP) on the DUT is measured between heating pulses. A front-end 16-bit analog-to-digital (AD) converter with a sequential output converts measurable voltage to digital code, which arrives at the MCU. The AD converter interacts with the MCU by means of high-speed serial interface, SPI. The measurement results are stored in the *memory* of the MCU. As the measurements are finished, the resulting data are transmitted to the computer for postprocessing. The MCU interacts with the computer through a USB-interface.

To determine the voltage temperature coefficient, k_T, the dependence of the forward voltage, *U,* of the solar module on its temperature, *T*, was measured. The measurements were taken at a measuring current, I_m, of 10 mA, with temperatures from 25–70 °C.

The measurement results showed that the dependence of voltage, *U*, on temperature, *T*, is linear, with a tangent slope angle, which defines k_T, equal to 45.8 mV/K.

IV. Results and Discussion

The measurement results for the variable temperature component *T*(*t*) of the die active area of the solar module obtained at various heating currents are shown in Fig. 3. Fig. 3(a) shows the time dependence of the heating pulse length, $\tau_p(t)$, which determines the harmonic modulation of the heating power. The modulation frequency of the heating power was set to 5 Hz. Dependencies of *T*(*t*) in Fig. 3(b)–(d) were obtained at heating currents of 250, 1000, and 2000 mA, respectively. The red colour shows the initial *T*(*t*) dependencies, and the black colour shows the digitally filtered dependencies. Voltage values, U_h, at the top of the heating pulses are 20.3, 22.3, and 23.6 V, respectively. Even though the power values dissipated in the device $(P = I_h U_h)$ significantly differ from each other (5.1, 22.3, and 47.2 W), the values of the variable component of temperature, T_1, are approximately the same in all cases (0.12, 0.15, and 0.15 °C). It should be noted that the quality of the signal that

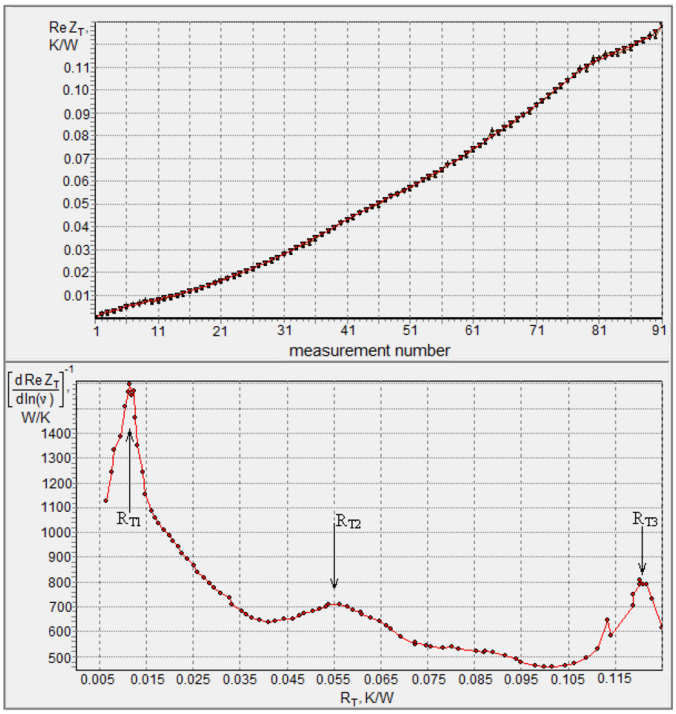

Fig. 4. Measurement results of thermal resistance components for the solar module at $I_h = 1000$ mA. Top: frequency dependence. Bottom: differential function that helps identify thermal resistance components.

determines transition temperature, $T(t)$, at $I_h = 250$ mA is much higher than it is at higher values of I_h.

To determine thermal resistance components of the solar module, the dependence of thermal impedance, $Z_T(\nu)$, on modulation frequency, ν, was measured. The frequency dependence of the thermal impedance real part, Re $Z_T(\nu)$, is shown in the upper graph in Fig. 4. A measurement counting number is plotted along the abscissa axis; the modulation frequency, ν, is decreased uniformly in the logarithmic frequency scale (20 measurements per decade). So, the modulation frequency for the first measurement was 100 Hz, and for the last one (number 91), it was 0.0032 Hz.

To identify the features of the Re $Z_T(\nu)$ dependence, it was differentiated with respect to ln(ν), which was followed by calculating the $[d\mathrm{Re}Z_T/d(\ln(\nu))]^{-1}$ function, which depends on thermal resistance R_T. The result is shown in the lower graph in Fig. 4. The peak positions relative to the R_T axis determine the thermal resistance components. Three peaks are clearly observed for the solar module DUT corresponding to three components: $R_{T1} = 0.0115$ K/W, $R_{T2} = 0.055$ K/W, and $R_{T3} = 0.121$ K/W. The R_{T2} component corresponds to the "junction-to-case" thermal resistance of the solar module at a modulation frequency of 0.5 Hz; component R_{T3} corresponds to the "junction-to-frame" thermal resistance at a modulation frequency of 0.01 Hz.

The R_{T1} component appears at a modulation frequency of 35 Hz. The reason for this component appearing is the large surface of the solar module and, therefore, nonhomogeneity of the current distribution through the p-n junction. Because of the p-n-junction's large area, which is approximately 4×10^5 mm^2

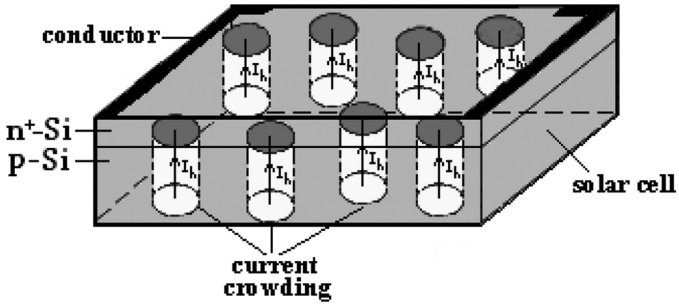

Fig. 5. Simplified solar module model with nonuniform current distribution through the p-n junction.

for the solar module, the current density j through the junction at $I_h = 1$ A is only 2.5 μA/mm^2, and at $I_h = 0.25$ A, it is four times smaller. With such a small value of j, the total forward current through the p-n junction consists of diffusion and recombination components. Both components of the current increase with the increase in temperature [13]. If at some point the p-n-junction current density, j, and power, P, increase, this leads to a local increase in transition temperature, ΔT_j, increase in the current density and a further local increase in temperature. Thus, due to the presence of positive thermal feedback, current crowding occurs, which was noted by Plesz *et al.* [5].

As local current nonhomogeneities, which are shown in Fig. 5 in yellow, arise in the solar module, this causes local areas of transition temperature, ΔT_j, and overheating relative to the rest of the module's semiconductor material. The local overheating is characterized by thermal resistance component R_{T1}. With an increasing I_h, the areas of local overheating increase in size. An increase in the surface area separating the areas of local overheating and the rest of the semiconductor material should lead to a decreasing thermal resistance R_{T1}. The results presented in Fig. 3 suggest that the local temperature increase, ΔT_j, remains essentially unchanged and dissipated power, P, increases with an increasing I_h. Consequently, the ratio $\Delta T_j/P$, which determines the thermal resistance of component R_{T1} according to (1), should decrease with an increasing I_h.

To test this assumption, thermal impedance, $Z_T(\nu)$, on the heating power modulation frequency, ν, dependencies for various heating currents, I_h were measured. The heating current was set in the range of 250–2500 mA, with 250 mA steps. The minimal heating power modulation frequency was 0.1 Hz, which made it possible to measure two thermal resistance components: R_{T1} and R_{T2}. The measurement results and spectral dependence processing of the thermal impedance real part Re $Z_T(\nu)$ are shown in Fig. 6. For perception convenience, they are all displaced along the ordinate axis by a constant value of 500 W/K.

At all heating current values, the thermal resistance component R_{T1} is clearly observable and its value decreases from 0.027 K/W at $I_h = 250$ mA to 0.0021 K/W at $I_h = 2500$ mA. Thermal resistance component R_{T1} is sharp at currents $I_h > 1000$ mA; at low currents it is weak. Therefore, the inset with a larger scale shows the calculation results for the three smallest currents: 250, 500, and 750 mA.

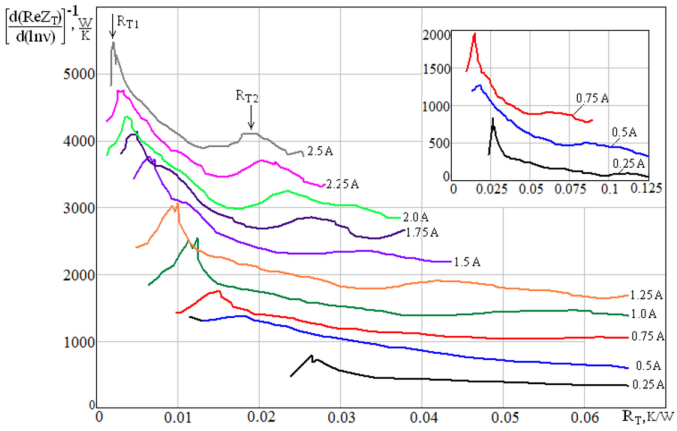

Fig. 6. Results of thermal resistance component measurement for the solar module with various heating currents I_h.

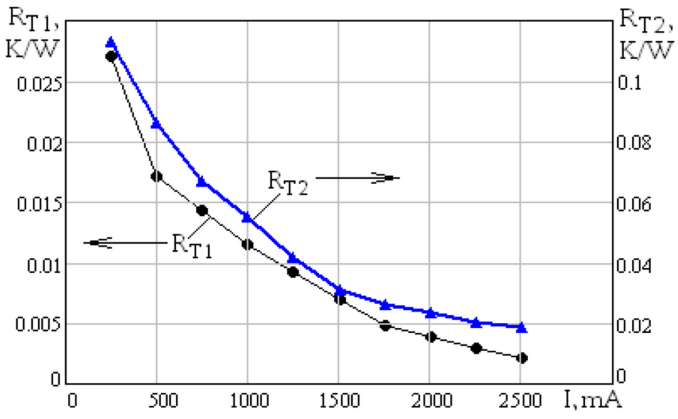

Fig. 7. Dependence of thermal resistance components values R_{T1} and R_{T2} on heating current I_h.

The dependence of thermal resistance components R_{T1} and R_{T2} on heating current is shown in Fig. 7. One can see that for both components, the $R_T(I_h)$ dependence is nonlinear, i.e., it decreases sharply in the area of small currents and tends toward a constant value at large currents. This dependence is confirmed by the literature [4], [5]. It should be noted that only the "transition-to-case" thermal resistance component was measured in the literature. The measurement objects had a relatively small surface area (16 and 38 cm^2), which is much smaller than the area of the module studied in this work (3800 cm^2). Therefore, it is possible to reach the values of heating current, I_h, at which thermal resistance, R_T, ceases to depend on I_h, which only occurs at substantially larger heating currents.

V. Conclusion

The measurements of the solar module thermal resistance revealed a distinctive feature associated with a large p-n-junction surface. In contrast to conventional semiconductor devices, such as diodes, transistors, and thyristors, an increase in the heating current in the module does not lead to an increase in the p-n-junction temperature. This is explained by the nonuniform current distribution through the junction and the formation of local heating areas in the semiconductor–current crowding. The occurrence of local heating areas was confirmed experimentally by detecting component R_{T1}, which appears due to a temperature difference between the local heating areas and the rest of the semiconductor. The occurrence of the local heating areas was also confirmed by the nonlinear thermal resistance components dependence on heating current, I_h. With an increasing I_h due to current crowding size increase, the degree of current distribution nonhomogeneity decreases and the thermal resistance ceases to depend on I_h.

References

[1] B. Siegal, Solar photovoltaic cell thermal measurement issues, *Presented at SEMI-THERM*, 2010, pp. 132–135. Accessed: Nov. 14, 2018. [Online]. Available: http://www.thermengr.com/Siegal_SPVC_Thermal_Issues.pdf

[2] O. Dupré, "Physics of the thermal behavior of photovoltaic devices," Thermics [physics.class-ph]. INSA de Lyon, 2015. Accessed: Nov. 14, 2018. Available: https://www.researchgate.net/publication/288670410_Physics_of_the_thermal_behavior_of_photovoltaic_devices

[3] S. H. Jang and M. W. Shin, "Thermal characterization of junction in solar cell packages," *Electron. Device Lett.*, vol. 31, no. 7, pp. 743–745, 2010.

[4] J. Zhang *et al.*, "Transient thermal resistance test of single-crystal-silicon solar cell," *IEEE Trans. Electron. Devices*, vol. 59, no. 9, pp. 2345–2349, Sep. 2012.

[5] B. Plesz, S. Ress, P. G. Szabó, G. Hantos, and D. Dudola, "Issues of thermal transient testing on photovoltaic modules presented at thermal investigations of ICs and systems (Therminic)," in *Proc. 20th Int. Workshop Therm. Investig. ICs Syst.*, 2014, pp. 1–5.

[6] G. De Mey, J. Wyrzutowicz, A. De Vos, W. Maranda, and A. Napieralski, "Influence of lateral heat diffusion on the thermal impedance measurement of photovoltaic panels," *Sol. Energy Mater. Sol. Cells*, vol. 112, pp. 1–5, May 2013.

[7] *Methodology for the Thermal Measurement of Component Packages (Single Semiconductor Device)*, JEDEC standard JESD51 1-14, pp. 2005–2010, 2010.

[8] Mentor Graphics Ltd. *T3Ster—Thermal Transient Tester—Technical Information*, 2018. Accessed: Jan. 3, 2018. [Online]. Available: https://www.mentor.com/products/mechanical/micred/

[9] Cold Plates, *Lytron Total Thermal Solutions*, 2018. Accessed: Jan. 4, 2018. [Online]. Available: http://www.lytron.com/Cold-Plates

[10] V. Smirnov, V. Sergeev, and A. Gavrikov, "Apparatus for measurement of thermal impedance of high-power light-emitting diodes and LED assemblies," *IEEE Trans. Electron. Devices*, vol. 63, no. 6, pp. 2431–2435, Jun. 2016.

[11] V. I. Smirnov, V. A. Sergeev, A. A. Gavrikov, and A. M. Shorin, "Modulation method for measuring thermal impedance components of semiconductor devices," *Microelectron. Reliab.*, vol. 80, pp. 205–212, Jan. 2018.

[12] V. Smirnov, V. Sergeev, A. Gavrikov, and A. Shorin1, "Thermal impedance meter for power MOSFET and IGBT transistors," *IEEE Trans. Power Electron.*, vol. 33, no. 7, pp. 6211–6216, Jul. 2018, doi: 10.1109/TPEL.2017.2740961.

[13] S. M. Sze and K. K. Ng, *Physics of Semiconductor Devices*. Hoboken, NJ, USA: Wiley, 2006.

Authors' photographs and biographies not available at the time of publication.